

0017-9310(94)E0064-2

# Onset of oscillatory convection in binary mixtures with Sorét effects and solidification

CHRISTIAN KARCHER and ULRICH MÜLLER

 Kernforschungszentrum Karlsruhe GmbH, Institut für Angewandte Thermo- und Fluidodynamik,  
 Postfach 36 40, D-76021 Karlsruhe, Germany

(Received 1 October 1993 and in final form 24 February 1994)

**Abstract**—The oscillatory instability of convection in a binary liquid-mixture with negative Sorét effects coupling Bénard convection and solidification is investigated when the temperature of the upper boundary is below the freezing point of the two-component system. Complete rejection of the lean component from the solid into the liquid phase is assumed. The Sorét coefficient and the coefficients of thermal and solutal expansion depend strongly on the local concentration in the liquid and, consequently, on the thickness of the solidified layer. Linear stability analysis for typical ethanol–water mixtures demonstrates that the variation of concentration is a dominant effect in the destabilization of the conductive state.

## 1. INTRODUCTION

WE STUDY the convective instability of a binary liquid-layer heated from below and cooled from above so that in the basic state of heat conduction a planar solid–liquid interface separates ice in the upper part of the layer from liquid below (see Fig. 1). During solidification the solute is assumed to be completely rejected into the liquid phase and, therefore, the solid consists of pure solvent. Moreover, in the liquid mixture negative Sorét effects are present. Hence, the imposed temperature gradient induces a stabilizing concentration gradient across the height of the liquid layer. In such a system beyond a certain critical temperature difference the basic state is replaced by oscillatory convection.

In the absence of phase transformation the influence of negative Sorét effects on convection in binary mixtures was first studied theoretically by Hurle and Jakeman [1, 2], Platten [3] and Velarde and Schechter [4]. These authors considered a simplified case in which thermal diffusion effects result in a linear concentration profile of the basic state. Chock and Li

[5] and more recently Zimmermann [6] based their stability analyses on a more general balance equation describing the mass flux in binary mixtures. Further investigations of this problem have been carried out by Linz and Lücke [7], Knobloch and Moore [8] and Cross and Kim [9]. The main result of all these analyses is that for sufficiently negative Sorét numbers  $S$ , characterized by  $S < S_{CT}$  and  $S_{CT} < 0$ , the basic state becomes initially unstable to oscillatory perturbations as the temperature difference across the layer exceeds a critical value. When  $S > S_{CT}$  a steady-state instability occurs. The case  $S = S_{CT}$  denotes the codimension-two point where both instabilities coexist at the same critical value.

In the presence of a solid–liquid interface there are, to our knowledge, only two papers dealing with the stability of a binary mixture subject to negative Sorét effects. Zimmermann *et al.* [10] and Karcher [11] find for sufficiently negative Sorét numbers an oscillatory onset of convection. These authors assume in their analysis that the fluid properties are independent of the changing mean concentration within the liquid. However, Kolodner *et al.* [12] have shown that the

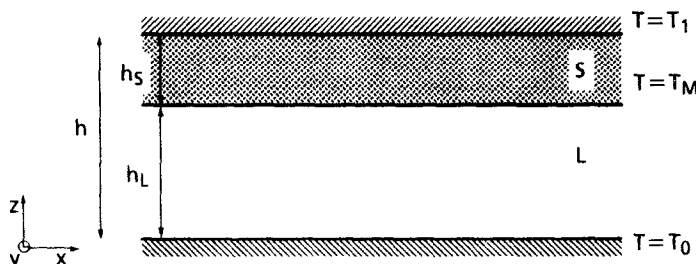


FIG. 1. Principle sketch.

## NOMENCLATURE

$A$	height ratio, $h_s/h_L$	$W$	vertical velocity
$C$	concentration [wt fr.]	$z$	vertical coordinate.
$C_0$	initial concentration	Greek symbols	
$c_p$	heat capacity [ $\text{kJ kg}^{-1} \text{K}^{-1}$ ]	$\alpha$	thermal expansion coefficient [ $\text{K}^{-1}$ ]
$D_0$	molecular diffusivity [ $\text{m}^2 \text{s}^{-1}$ ]	$\alpha'$	solutal expansion coefficient [wt fr. $^{-1}$ ]
$g$	acceleration of gravity [ $\text{m s}^{-2}$ ]	$\kappa$	thermal diffusivity [ $\text{m}^2 \text{s}^{-1}$ ]
$h$	layer height [m]	$\nu$	kinematic viscosity [ $\text{m}^2 \text{s}^{-1}$ ]
$H$	amplitude of the interface deflection	$\rho$	density [ $\text{kg m}^{-3}$ ]
$i$	imaginary unit	$\lambda$	thermal conductivity [ $\text{W m}^{-1} \text{K}^{-1}$ ]
$J$	mass flux	$\omega$	frequency
$k$	wave number	$\tau$	oscillation period [s]
$L$	latent heat of the solvent [ $\text{kJ kg}^{-1}$ ]	$\psi$	separation ratio, $SR_S C^*(1 - C^*)$ .
$Le$	Lewis number, $D_0/\kappa^{(L)}$	Superscripts	
$m$	slope number, $m' \Delta T_L^{-1}$	$*$ , $-$	mean value, value in the basic state
$m'$	slope of the melting curve [K]	(os)	oscillatory
$Pr$	Prandtl number, $\nu/\kappa^{(L)}$	L, S	liquid, solid.
$Ra$	Rayleigh number, $\alpha g \Delta T_L h_L^3 / (\kappa^{(L)} \nu)$	Subscripts	
$R_S$	expansion ratio, $(\alpha'/\alpha) \Delta T_L^{-1}$	c	critical
$S$	Sorét number, $S_T \Delta T_L$	CT	codimension-two
$S_T$	Sorét coefficient [ $\text{K}^{-1}$ ]	eff	effective
$Sc$	Schmidt number, $\nu/D_0$	L, S	liquid, solid
$Ste$	Stefan number, $L/(c_p \Delta T_L)$	0, 1	upper, lower boundary.
$t$	time [s]		
$T$	temperature		
$T_M$	melting temperature		
$\Delta T$	temperature difference		

Sorét coefficient  $S_T$  in a water–ethanol mixture depends strongly on the concentration of the mixture, see Fig. 2. Moreover, a thorough analysis of density data of D'Ans-Lax [13] demonstrates that also the coefficients of thermal and solutal expansion,  $\alpha$  and  $\alpha'$ , vary strongly with the local alcohol concentration. This is shown in Fig. 3 for a mixture at a mean temperature  $T^* = 5^\circ\text{C}$ . These variations are relevant in the present problem since during solidification complete rejection of the solute into the liquid phase is assumed. Hence, increasing the ice thickness leads to an increase of the mean concentration within the liquid.

In the present paper we include the effect of a varying mean concentration on the onset of oscillatory convection in a binary mixture with negative Sorét effects as influenced by a solid–liquid interface. In particular, in the stability analysis we take into account concentration-dependent coefficients  $S_T$ ,  $\alpha$  and  $\alpha'$ . We also perform a re-evaluation of the experimental data of Zimmermann *et al.* [10], by accounting more accurately for the variations of the fluid properties with concentration and temperature.

## 2. FORMULATION OF THE PROBLEM

We consider the basic state of heat conduction in a partly solidified two-component layer (see Fig. 1). The

layer is heated from below at  $z = 0$  and cooled from above at  $z = h$  by arranging a temperature difference  $\Delta T = T_1 - T_0$  between bottom and top. The temperature at the top is below the freezing point of the mixture. Thus there is a solidified layer of pure solvent of height  $h_s$  above a binary liquid-layer of height  $h_L$ . The temperature difference across the liquid phase is  $\Delta T_L = T_0 - T_M$ , with  $T_M$  the concentration-dependent melting temperature. Due to the presence of a negative Sorét coefficient  $S_T$  of the mixture, a stabilizing distribution of the concentration  $\bar{C}(z)$  is induced. The initial concentration is denoted by  $C_0$ , defined in the ice-free case. Further properties of the liquid are the thermal diffusivity  $\kappa^{(L)}$ , molecular diffusivity  $D_0$ , kinematic viscosity  $\nu$  and heat capacity  $c_p$ .

The stability of the basic state is governed by the linearized Boussinesq equations within the liquid together with boundary conditions at the bottom  $z = 0$  and appropriate interfacial conditions at  $z = h_L$ . The corresponding eigenvalue problem for the onset of convection was derived in detail in ref. [10] and will only be briefly presented here. The non-dimensional perturbation equations for the  $z$ -dependent normal-mode amplitudes of the vertical velocity  $W$ , temperature  $T$ , concentration  $C$  and mass flux  $J$  read as:

$$(D^2 - k^2)(D^2 - k^2 + i\omega Pr)W - Rak^2[T + R_S C_0 C] = 0, \quad (1)$$

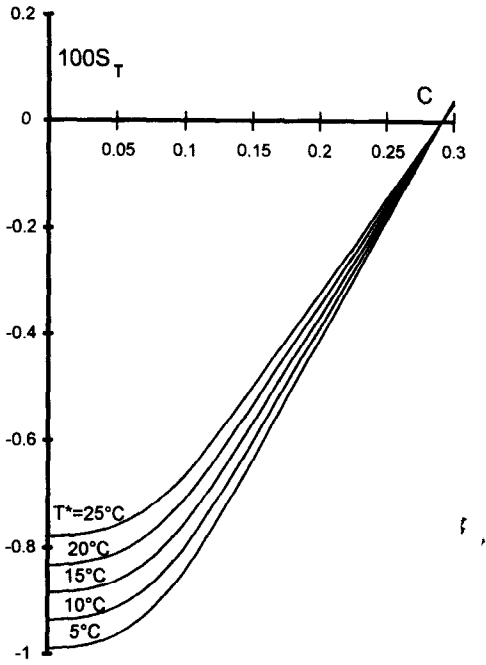


FIG. 2. Sorét coefficient  $S_T$  of a water-ethanol mixture as function of ethanol concentration  $C$  and mean temperature  $T^*$  according to Kolodner *et al.* [12].

$$(D^2 - k^2 + i\omega)T + W = 0, \quad (2)$$

$$-DJ + Sc Pr^{-1} [i\omega C - (D\bar{C})W] - k^2 [C - S\bar{C}(1 - C_0\bar{C})T] = 0, \quad (3)$$

$$J = -DC + S[\bar{C}(1 - C_0\bar{C})DT - (1 - 2C_0\bar{C})C]. \quad (4)$$

Here  $D$  represents the derivative with regard to the vertical direction,  $k$  is the horizontal wave number of the normal modes, and  $\omega$  denotes the frequency of oscillations. We have used the scales  $h_L$ ,  $h_L^2/\kappa^{(L)}$ ,  $\kappa^{(L)}/h_L$ ,  $\Delta T_L$  and  $C_0$  for length, time, velocity, temperature difference and concentration, respectively.

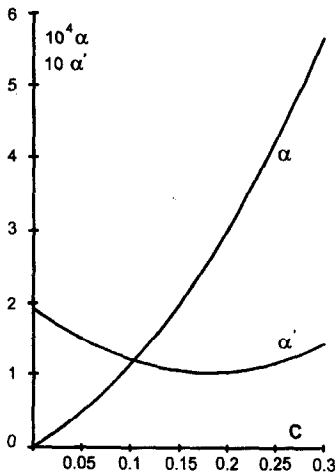


FIG. 3. Coefficients of thermal and solutal expansion,  $\alpha$  and  $\alpha'$ , of a water-ethanol mixture as function of ethanol concentration  $C$  at mean temperature  $T^* = 5^\circ\text{C}$  according to density data of D'Ans-Lax [13].

The lower boundary is rigid, perfectly conducting and impermeable. Thus we have:

$$W = DW = T = J = 0 \quad \text{at } z = 0. \quad (5)$$

At the solid-liquid interface we have to fulfil the conservation equations of mass, energy and solute. Furthermore the no-slip condition holds. These conditions are:

$$W + i\omega(1 - \rho)H = 0, \quad (6)$$

$$DT + \lambda\delta \text{cth}(\delta A)T + [(\lambda - 1)\delta \text{cth}(\delta A) - i\omega\rho Ste]H = 0, \quad (7)$$

$$J + i\omega\rho Sc Pr^{-1} \bar{C}H = 0, \quad (8)$$

$$DW = 0 \quad \text{at } z = 1, \quad (9)$$

where:

$$\delta = (k^2 - i\omega\kappa^{-1})^{1/2}. \quad (10)$$

In the interfacial conditions (6)–(8),  $H$  represents the normal-mode amplitude of the deflection of the interface at  $z = 1$ , given by:

$$H = (T - mC_0C)[1 + mC_0(D\bar{C})]^{-1}. \quad (11)$$

The basic state is characterized by a linear temperature profile and a non-linear concentration distribution [10]. We find:

$$\bar{T}(z) = 1 - z, \quad (12)$$

$$\bar{C}(z) = \{C_0 + (1 - C_0\bar{C}_{(1)})\bar{C}_{(1)}^{-1} \exp[S(1 - z)]\}^{-1}, \quad (13)$$

where the interfacial concentration is:

$$\bar{C}_{(1)} = \frac{\exp[C_0(1 + A)S] - 1}{C_0(\exp[S] - 1)}. \quad (14)$$

Equations (13) and (14) imply the assumption of complete rejection of solute during solidification.

The eigenvalue problem defined above is controlled by a set of 12 parameters. The relevant dimensionless groups for describing the main physical phenomena are the Rayleigh number  $Ra$ , the expansion ratio  $R_S$ , the height ratio  $A$ , the Sorét number  $S$ , and the initial concentration  $C_0$ , given by the expressions:

$$Ra = \frac{\alpha g \Delta T_L h_L^3}{\kappa^{(L)} \nu}, \quad R_S = \frac{\alpha'}{\alpha \Delta T_L},$$

$$A = \frac{h_S}{h_L}, \quad S = S_T \Delta T_L, \quad C_0. \quad (15a) - (15e)$$

Other relevant parameters are the Prandtl number  $Pr$ , the Schmidt number  $Sc$ , the Stefan number  $Ste$ , the slope number  $m$ , and the solid-liquid ratios of reference density  $\rho$ , thermal conductivity  $\lambda$ , and thermal diffusivity  $\kappa$ :

$$Pr = \frac{\nu}{\kappa^{(L)}}, \quad Sc = \frac{\nu}{D_0}, \quad Ste = \frac{L}{c_0 \Delta T_L},$$

Table 1. Sorét number  $S$  and expansion ratio  $R_S$  as function of the height ratio  $a$  for a typical water–ethanol mixture with initial concentration  $C_0 = 0.15$  at mean temperature  $T^* = 5^\circ\text{C}$

$A$	0	0.01	0.02	0.04	0.06	0.08	0.1
$S$	-0.1624	-0.1608	-0.1591	-0.1557	-0.1522	-0.1488	-0.1454
$R_S$	24.9	24.33	23.78	22.74	21.8	20.92	20.12
$A$	0.12	0.16	0.2	0.24	0.28	0.32	0.36
$S$	-0.1419	-0.1350	-0.1281	-0.1212	-0.1143	-0.1073	-0.1004
$R_S$	19.38	18.05	16.9	15.91	15.04	14.28	13.62

$$m = \frac{m'}{\Delta T_L}, \quad \rho = \frac{\rho_0^{(S)}}{\rho_0^{(L)}}, \quad \lambda = \frac{\lambda^{(S)}}{\lambda^{(L)}}, \quad \kappa = \frac{\kappa^{(S)}}{\kappa^{(L)}}. \tag{16a} \tag{16g}$$

Here  $L$  is the latent heat of the solvent, and  $m'$  denotes the slope of the melting curve of an ideal mixture (see Ott *et al.* [14]).

3. METHOD OF SOLUTION

3.1. Calculation procedure

Using the basic equations of the previous chapter we calculate the critical Rayleigh number  $Ra_c^{(os)}$  and the critical frequency  $\omega_c$  for the onset of oscillatory convection as the height ratio  $A$  is varied. The calculation procedure is as follows: for a given  $A$  and a corresponding increased concentration of solute in the liquid phase we define the mean concentration  $C^* = C_0(1 + A)$  within the liquid. The initial concentration and the mean temperature are fixed at values  $C_0 = 0.15$  and  $T^* = 5^\circ\text{C}$ , which correspond to the experimental conditions of Zimmermann *et al.* [10]. Then we calculate the parameter  $S = S(C^*)$  using data for  $S_T$  as shown in Fig. 1 and a first estimation of  $\Delta T_L$ . Now the melting temperature  $T_M(^{\circ}\text{C})$  can be derived from the relation  $T_M = m' C_0 \bar{C}_{(1)}$ , where we have  $\bar{C}_{(1)}$  from equation (14) and  $m'$  from the phase diagram [14]. Finally, we estimate  $\Delta T_L$  anew by setting  $\Delta T_L = 2(T^* - T_M)$  and repeat the calculational steps. As a result of the iteration we obtain the temperature profile of the basic state  $\bar{T}(z)$  ( $^{\circ}\text{C}$ ) to high accuracy. However, at low mean values the temperature profile gives rise to a non-linear density stratification within the liquid [6, 10]. To account for these non-Boussinesq effects we introduce integral mean definitions for the coefficients of thermal and solutal expansion by the expressions:

$$\alpha = - \int_0^1 \frac{1}{\rho} \frac{\partial \rho(T, C)}{\partial T} \Big|_{C^*, T(z)} dz, \tag{17}$$

$$\alpha' = - \int_0^1 \frac{1}{\rho} \frac{\partial \rho(T, C)}{\partial C} \Big|_{C^*, T(z)} dz, \tag{18}$$

where we take the density data from D'Ans-Lax [13]. These integral mean values are used to calculate the expansion ratio  $R_S(C^*)$ . In Table 1 we have listed the data of our evaluation. The absolute value of both

parameters, the Sorét number and the expansion ratio, obviously decrease as  $A$  increases.

All the other parameters are fixed at values likewise adapted to the experimental situation of Zimmermann *et al.* [10], i.e.  $Pr = 29.6$ ,  $Sc = 1027.7$ ,  $Ste = 3.02$ ,  $m = -1.96$  and  $\rho = \kappa = \lambda = 1.001$ . For this particular set of parameters the eigenvalue problem defined by equations (1)–(14) is solved numerically using the SUPORE code of Scott and Watts [15]. For comparison with previous results and for distinguishing the various physical effects we also repeat the calculations for parameters  $S$  and  $R_S$  independent of concentration [10, 11].

3.2. Re-evaluation of experimental results

The experiments of Zimmermann *et al.* [10] were performed in a rectangular large aspect-ratio cell of dimension length : width : height = 200 : 20 : 3.12 mm. The test liquid was a water–ethanol mixture with initial concentration  $C_0 = 15 \text{ wt\%}$ . Table 2 shows the experimental data. The measured quantities are the temperatures  $T_0$  and  $T_1$  at the lower and upper boundary, the mean ice thickness  $h_s$  and the period of oscillation  $\tau$ (s).

Our evaluation procedure is as follows: for each data sequence we calculate the liquid height  $h_L = h - h_s$ , the height ratio  $A = h_s/h_L$  and the mean concentration  $C^* = C_0(1 + A)$  within the liquid. To

Table 2. Experimental data of Zimmermann *et al.* [10] for a water–ethanol mixture with initial concentration  $C_0 = 15 \text{ wt\%}$

$T_0$ ( $^{\circ}\text{C}$ )	$T_1$ ( $^{\circ}\text{C}$ )	$h_s$ (mm)	$\tau$ (s)
15.56	-7.87	0	31.2
15.91	-8.51	0.035	30.6
16.97	-9.05	0.11	29.3
16.95	-9.5	0.18	28.8
18.79	-10.38	0.3	26.3
19.28	-10.41	0.32	26.1
20.17	-11.44	0.42	24.2
21.13	-11.78	0.45	24.6
21.57	-12.51	0.55	23.3
22.51	-13.14	0.59	22.1
24.37	-14.57	0.74	20.6
25.29	-15.27	0.78	19.3
25.74	-15.93	0.83	18.6
26.65	-16.65	0.87	18.6
26.17	-16.42	0.89	19.4

evaluate  $Ra_c^{(os)}$  from equation (15a) we need  $\Delta T_L$  and  $\alpha$  as further data input. This is done in the same way as described in Section 3.1. Thus we account more accurately for the fluid properties variation with  $C^*$  and the non-Boussinesq effects of the density–temperature relation. In the evaluation of Zimmermann *et al.* [10] both effects were neglected. To obtain the dimensionless frequencies of oscillation  $\omega_c$  from the experimental data we evaluate the scaling relation  $\omega_c = 2\pi^2 h_L^2 / (\kappa^{(L)} \tau)$ . By comparing dimensionless quantities we are able to separate different physical effects.

#### 4. RESULTS AND CONCLUSIONS

Figure 4 shows the critical Rayleigh numbers  $Ra_c^{(os)}$  for the onset of oscillations as function of the height ratio  $A$ . The results of our present analysis, which includes proper modelling of the solidification process with stepwise adjusted parameters  $S$  and  $R_S$  corresponding to Table 1, are characterized by symbols  $\diamond$ . In addition the calculated data based on the assumption of constant parameters [10, 11], i.e.  $S = -0.1624$  and  $R_S = 24.9$  defined at  $A = 0$ , are

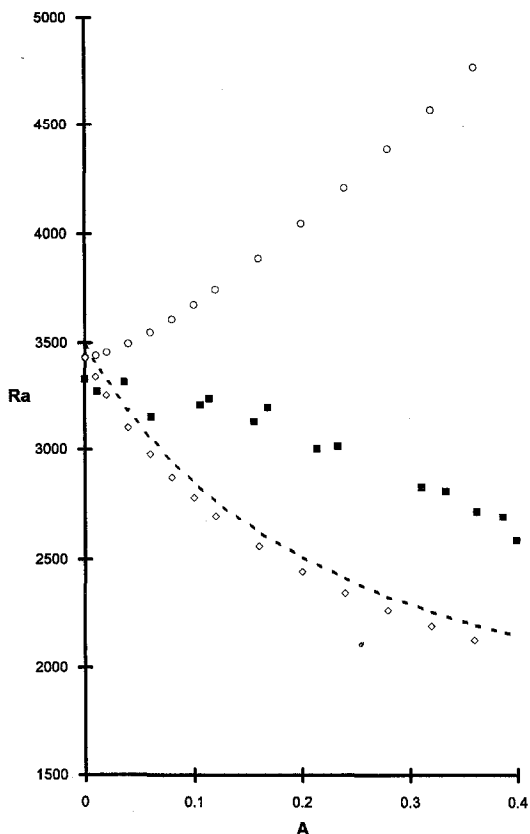


FIG. 4. Critical Rayleigh numbers for onset of oscillatory convection:  $\blacksquare$ —re-evaluated experimental values according to Zimmermann *et al.* [10];  $\diamond$ —calculated values for  $S(C^*)$  and  $R_S(C^*)$ ;  $\circ$ —calculated values for constant  $S$  and  $R_S$ ; (---)—evaluated curve according to the relation of Hurle and Jakeman [2].

given by symbols  $\circ$ . The re-evaluated experimental data of Zimmermann *et al.* [10] are denoted by symbols  $\blacksquare$ . In the experiments a decrease of  $Ra_c^{(os)}$  with increasing dimensionless ice layer thickness is observed.

The present calculations show that the theoretical assumption of parameters independent of concentration fails to describe the experimental results; the values of  $Ra_c^{(os)}$  increase monotonically with increasing  $A$  (see Fig. 4, symbols  $\circ$ ). This theoretical finding is inconsistent with the experiments, but can be explained as follows: increasing the ice thickness results in an effective Sorét number  $S_{\text{eff}}$  according to the relation  $S_{\text{eff}} = SC_0(1+A)$ , cf. equation (14). Hence, by fixing  $S$  and increasing  $A$ , negative Sorét effects are intensified leading to a stabilization of the liquid layer. This effect outweighs the destabilizing effect of the insulating ice layer. Note that the numerical results of Zimmermann *et al.* [10] presented in their Fig. 9a are incorrect (cf. ref. [10]).

A more realistic description of the experimental observations is obtained if the variation of  $C^*$  with both parameters—the Sorét number  $S$  and the expansion ratio  $R_S$ —is taken into account (see Fig. 4, symbols  $\diamond$ ). The calculated critical values decrease monotonically with increasing  $A$  and thus show qualitative agreement with the experiments. This behavior is directly related to the decrease of the absolute values of  $S$  and  $R_S$  as the ice layer becomes thicker (cf. data of Table 1). Thereby, the stabilizing effect of the concentration stratification is diminished and the critical Rayleigh numbers are reduced.

This result is supported by an approximate relation for the critical oscillatory Rayleigh number reported by Hurle and Jakeman [2]. This relation is given by:

$$Ra_c^{(os)} = Ra_{c0} \left( 1 - \frac{1.05\psi}{1 + \psi + Pr^{-1}} \right), \quad (19)$$

where  $Ra_{c0} = 1707.8$ . Equation (19) holds for binary liquid mixtures bounded above and below by rigid, perfectly conducting plates and in the limit of small or zero Lewis numbers  $Le = Pr Sc^{-1}$ . To evaluate the separation ratio  $\psi$  we use the data of Table 1 to account for the concentration dependence of the parameters, i.e.  $\psi = SR_S C^*(1 - C^*)$ . The critical Rayleigh numbers calculated by this method are given by the dotted line in Fig. 4. The values are slightly above those values denoted by symbols  $\diamond$ , which account for the solidification of solvent at the upper boundary. In fact, we attribute this small difference to the neglecting of solidification at the upper boundary when employing equation (19). Hence, the destabilizing effect of the insulating ice layer has only a minor influence on the onset of oscillatory convection.

There are still quantitative differences between the experimental data and the numerical findings for the case of varying parameters  $S$  and  $R_S$ . In the range  $0.1 < A < 0.4$  the critical Rayleigh numbers predicted by our analysis are about 20% smaller than

those of the experiments. We attribute this systematic deviation to uncertainties which arise from extrapolating the Sorét data of Kolodner *et al.* [12], valid in the range  $10^\circ\text{C} < T^* < 40^\circ\text{C}$ , to values at a mean temperature  $T^* = 5^\circ\text{C}$ , and from extrapolating likewise density data of D'Ans-Lax [13] for  $T \geq 0^\circ\text{C}$  to a range  $T_M \leq T \leq 0^\circ\text{C}$ . Moreover, the use of an averaging procedure for  $S$  and  $R_S$  rather than using their local functional properties in the basic equations may also give rise to a deviation.

Figure 5 shows the dependence of the critical frequency of oscillation  $\omega_c$  on the height ratio  $A$ . We have used the same symbols as in Fig. 4 to denote the different theoretical approaches and the re-evaluated experimental data of Zimmermann *et al.* [10]. The graph shows that the experimental values decrease slightly for the whole parameter range  $0 < A < 0.4$ . Hence, the observed strong decrease of  $\tau$  with increasing  $h_S$  (cf. data of Table 2 and Figure 9b of ref. [10]) is mainly caused by the decrease of the liquid-layer height  $h_L$ .

The calculated frequency data based on the assumption of parameters  $S$  and  $R_S$  independent of concentration do not reflect the experimental findings (see

Fig. 5, symbols  $\circ$ ), as a monotonic increase of  $\omega_c$  with increasing  $A$  is predicted. The increase of the calculated values can be explained by the enhanced effective Sorét number  $S_{\text{eff}} = SC_0(1+A)$  in the presence of an ice layer.

If the variation of the parameters  $S$  and  $R_S$  with the ice thickness according to Table 1 is taken into account, the numerical results show a monotonic decrease of the critical frequencies with increasing height ratio  $A$  (see Fig. 5, symbols  $\diamond$ ). This feature is explained by the lessening of the negative Sorét effect due to an increasing mean concentration which results in lower frequencies.

A comparison of the calculated new data for varying parameters  $S$ ,  $R_S$  and the experimental values shows qualitative agreement as both data sequences decrease with increasing  $A$ . However, the theoretical values of  $\omega_c$  decrease significantly stronger than the experimental ones. Moreover, there is a discrepancy of about 10% in the calculated and observed frequency in a layer without ice ( $A = 0$ ). The existing discrepancy suggests that there are still some physical effects in the experiment which are not quantitatively accounted for in the model. Already above we pointed out three effects which may explain discrepancies for the calculated and observed critical Rayleigh numbers. These defects should apply for the frequency as well.

Finally, we evaluate the approximate relation of Hurle and Jakeman [2] for the critical frequency given as:

$$\omega_c = \frac{3}{2}\pi^2 1.43 \left( \frac{-\psi}{1+\psi+Pr^{-1}} \right)^{1/2}, \quad (20)$$

by adapting the separation ratio  $\psi$  to the actual mean concentration  $C^*$  within the liquid. The results are represented by the dotted line in Fig. 5. This curve is located distinctly above our calculated values denoted by symbols  $\diamond$  but both data sequences decrease monotonically for increasing height ratio  $A$ . Thus there is qualitative agreement. The existing difference between the two data sets is attributed to a decreasing accuracy of the approximate relation for large negative  $\psi$ -values as noticed already by Lhost *et al.* [16], and in particular to the fact that solidification effects at the upper boundary are included in our analysis while neglected in the derivation of equation (20).

In summary we conclude that the predominant influence of a solid-liquid interface on the oscillatory instability in a binary liquid mixture is the change of property parameters such as Sorét number  $S$  and expansion ratio  $R_S$  with a variation of the mean concentration in the liquid. This variation originates from a changing ice thickness since during solidification the light component is rejected into the liquid phase. Interfacial conditions like the insulating effect induced by the presence of the ice layer are of minor importance.

*Acknowledgements*—The authors would like to acknowledge helpful discussions with Prof. S. H. Davis, and Dr G. Zim-

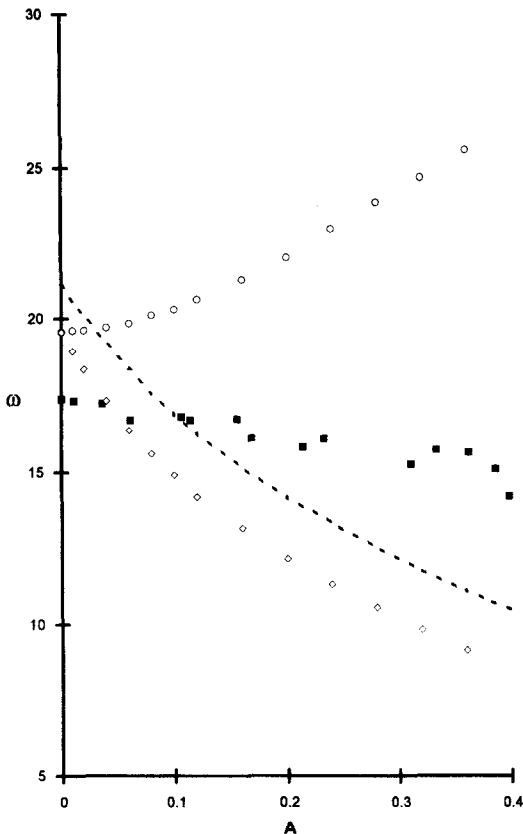


FIG. 5. Critical frequencies for onset of oscillatory convection: ■—re-evaluated experimental values according to Zimmermann *et al.* [10]; ◇—calculated values for  $S(C^*)$  and  $R_S(C^*)$ ; ○—calculated values for constant  $S$  and  $R_S$ ; (---)—evaluated curve according to the relation of Hurle and Jakeman [2].

mermann for providing his original experimental data. We also greatly appreciate useful comments by Professors D. T. J. Hurle and P. Kolodner.

### REFERENCES

1. D. T. J. Hurle and E. Jakeman, Significance of the Sorét effect in the Rayleigh–Jeffreys problem, *Phys. Fluids* **12**, 2704–2707 (1969).
2. D. T. J. Hurle and E. Jakeman, Sorét-driven thermosolutal convection, *J. Fluid Mech.* **47**, 667–687 (1971).
3. J. K. Platten, Le Problème de Bénard dans les mélanges : cas de surface libre, *Bull. Classe Sci. Acad. Roy. Belg.* **57**, 669–683 (1971).
4. M. Velarde and R. Schechter, Thermal diffusion and convective instability (III): a critical survey of Sorét coefficient measurements, *Chem. Phys. Lett.* **12**, 312–315 (1971).
5. D. P. Chock and C.-H. Li, Direct integration method applied to Sorét-driven instability, *Phys. Fluids* **18**, 1401–1406 (1975).
6. G. Zimmermann, Bénard–Konvektion in binären Flüssigkeitsmischungen mit Thermodiffusion, *KfK-Bericht* **4623** (1990).
7. S. Linz and M. Lücke, Convection in binary mixtures : a Galerkin model with impermeable boundary conditions, *Phys. Rev. A* **35**, 3997–4000 (1987).
8. E. Knobloch and D. R. Moore, Linear stability of experimental Sorét convection, *Phys. Rev. A* **37**, 860–870 (1988).
9. M. C. Cross and K. Kim, Linear instability and the codimension-2-region in binary fluid convection between rigid impermeable boundaries, *Phys. Rev. A* **37**, 3909–3920 (1988).
10. G. Zimmermann, U. Müller and S. H. Davis, Bénard convection in binary mixtures with Sorét effects and solidification, *J. Fluid Mech.* **238**, 657–682 (1992), and Corrigendum *J. Fluid Mech.* **254**, 720 (1993).
11. Ch. Karcher, Bénard–Konvektion binärer Flüssigkeitsmischungen in porösen Medien unter der Wirkung von Nicht-Boussinesq-Effekten, Ph.D. dissertation, Universität Karlsruhe (TH) (1993).
12. P. Kolodner, H. Williams and C. Moe, Optical measurement of Sorét coefficient of ethanol/water solutions, *J. Chem. Phys.* **88**, 6512–6524 (1988).
13. E. D’Ans-Lax, *Taschenbuch für Chemiker und Physiker*, Vol. 1 (3rd Edn). Springer-Verlag, Berlin (1967).
14. J. B. Ott, J. R. Goates and B. A. Waite, (Solid + liquid) phase equilibria and solid-hydrate formation in water + methyl, + ethyl, + isopropyl, and + tertiary butyl alcohols, *J. Chem. Thermodyn.* **11**, 739–746 (1979).
15. M. R. Scott and H. A. Watts, Subroutine SUPORE, Rep. Sand75-0198, Sandia Labs, Albuquerque (1975).
16. O. Lhost, S. J. Linz and H. W. Müller, Onset of convection in binary liquid mixtures : improved Galerkin approximations, *J. Phys. II* **1**, 279–287 (1991).